

Effects of Substituting La and Zn in Disordered $\text{Sr}_2\text{FeMoO}_6$

Le Duc Hien, Dao Thi Thuy Nguyet, Nguyen Phuc Duong*

Hanoi University of Science and Technology, No. 1, Dai Co Viet, Hai Ba Trung, Hanoi, Viet Nam

Received: August 10, 2017; Accepted: June 24, 2019

Abstract

The $\text{Sr}_{2-x}\text{La}_x\text{FeMoO}_6$ ($x = 0, 0.1, 0.2, 0.3, 0.4$) and $\text{Sr}_2\text{Fe}_{1-x}\text{Zn}_x\text{MoO}_6$ ($x = 0.05, 0.1, 0.15$) samples were prepared using a sol-gel route followed by heat-treatment. X-ray diffraction (XRD), field-emission scanning electron microscope (FESEM) were employed to characterize phase formation and morphology. Magnetization curves in the temperature range 88–430 K were measured by means of a vibrating sample magnetometer (VSM) from which the magnetic moment at 0 K and Curie temperature were determined. The antisite disorder in the samples was evaluated based on the magnetic moment data and the substitution levels. The effects of La and Zn substitution on the magnetic parameters were discussed.

Keywords: $\text{Sr}_2\text{FeMoO}_6$, La and Zn substitution, magnetization, Curie temperature, antisite disorder

1. Introduction

$\text{Sr}_2\text{FeMoO}_6$ (SFMO) belongs to the double perovskite family with half-metallic ground states in which conduction electrons are fully spin polarized and have ferromagnetic transition temperatures well above room temperature ($T_C > 400$ K). This material therefore draws a lot of attention for applications in the field of spintronics as spin injectors and tunneling magnetoresistance devices. The ideal structure of SFMO is a stacking of corner sharing FeO_6 and MoO_6 octahedral which alternate along three directions of the crystal and form the B and B' sublattices respectively, while the Sr cations occupy the vacant sites between octahedral. In the compound, the majority spin up channel ($t_{2g}\uparrow$ and $e_g\uparrow$) with a band gap is formed by 'localized' core spins of Fe^{3+} ($S = 5/2$) ions. On the other hand, the spin down $t_{2g}\downarrow$ states of Mo and Fe together with some small admixture of the O $2p$ states form a conduction band lying at the Fermi level [1]. This band exhibits a full negative polarization ($P = -1$) which is partially filled by $4d^1$ electrons of Mo^{5+} . The $e_g\downarrow$ levels of both Mo and Fe are empty. The Mo and Fe $t_{2g}\downarrow$ states are coupled via hopping interaction mechanism. Because the available Fe $t_{2g}\downarrow$ state is purely spin down polarized and due to Hund's rule, the electron hopping can only occur when the localized Fe spin moments are ferromagnetically aligned. The overall magnetic moment is well described by the ionic model of an antiferromagnetic arrangement between Fe^{3+} core spin and the Mo^{5+} $4d$ spin leading to the net moment of $4 \mu_B$ per formula unit. However, in real materials a certain degree of antisite disorder (AS)

often exists in which some of Mo ions occupy the Fe ion sites and vice versa hence the saturation magnetization is often lower than the predicted value.

As ferromagnetism in half metallic double perovskites is mediated by itinerant carriers, it is expected that the magnetic properties are sensitive to substitutional elements with different valences, for instance, substituting Sr^{2+} by La^{3+} or replacing Fe^{3+} by a divalent cation such as Zn^{2+} . There are a number of studies on $\text{Sr}_{2-x}\text{La}_x\text{FeMoO}_6$ and $\text{Sr}_2\text{Fe}_{1-x}\text{Zn}_x\text{MoO}_6$ series were implemented [2–7]. In these works, the influence of substitution effect on saturation magnetization, Curie temperature was investigated. However, these parameters are also affected by the concentration of anti-site defects which on the other hand depends on heat-treatment conditions and concentration of substitutional elements. Usually, in order to obtain SFMO sample with AS of less than 10%, an annealing process in a reduction atmosphere and at high temperatures ($\sim 1200^\circ\text{C}$) is required [2,4,7].

This paper is aimed to provide further information on the interplay of doping and AS effects in magnetic properties of $\text{Sr}_{2-x}\text{La}_x\text{FeMoO}_6$ and $\text{Sr}_2\text{Fe}_{1-x}\text{Zn}_x\text{MoO}_6$ samples prepared by using sol-gel technique followed by heat-treatment at lower annealing temperature.

2. Experimental

In the sol-gel procedure, aqueous solutions of $(\text{NH}_4)_6\text{Mo}_7\text{O}_{24}\cdot 4\text{H}_2\text{O}$, $\text{Fe}(\text{NO}_3)_3\cdot 9\text{H}_2\text{O}$, $\text{Sr}(\text{NO}_3)_2$, and $\text{La}(\text{NO}_3)_3$ or $\text{Zn}(\text{NO}_3)_2$ were prepared by dissolving stoichiometric amounts in deionized water. Firstly, solutions of $\text{Fe}(\text{NO}_3)_3\cdot 9\text{H}_2\text{O}$, $\text{Sr}(\text{NO}_3)_2$ and $\text{La}(\text{NO}_3)_3$ or $\text{Zn}(\text{NO}_3)_2$ were mixed together with citric acid. Solution of $(\text{NH}_4)_6\text{Mo}_7\text{O}_{24}\cdot 4\text{H}_2\text{O}$ was then added to

* Corresponding author: Tel.: (+84) 903.291.281
Email: nguyet@itims.edu.vn

obtain the final solution in which the molar ratios between metal ions are set according to the chemical formula of $\text{Sr}_{2-x}\text{La}_x\text{FeMoO}_6$ or $\text{Sr}_2\text{Fe}_{1-x}\text{Zn}_x\text{MoO}_6$. The molar ratio of the total amount of metal cation to the citric acid amount is 1:3. The obtained solution was magnetically stirred at 80°C till the liquid turned to a gel. The gel was dried at 110°C for 24 h, then ground and heated at 500°C for 2 h. The powder portions were pressed into pellets under pressure of 2.5 tons/cm² and were annealed at high temperatures under stream of H₂/Ar mixed gas (15 vol% H₂) with flow rate of 10 sccm at 1100°C for 8 h.

X-ray powder diffraction (XRD) data were collected with a Siemens D5000 (CuK α radiation, $\lambda = 1.54056 \text{ \AA}$) to identify the crystal structure. Field Emission-Scanning Electron Microscopy (FESEM) (JEOL JSM-7600 F) was used to examine the grain size and morphology. Magnetization curves were measured using a vibrating sample magnetometer (VSM) (MicroSense EZ9) in the temperature range of 88–430 K and applied magnetic fields up to 10 kOe.

3. Results and discussion

The XRD patterns measured for all the samples can be well indexed using the tetragonal $I4/m$ space group and indicate that the samples are in single phase. The lattice parameters a and c were determined based on the XRD data and are shown in Fig. 1. For the $\text{Sr}_{2-x}\text{La}_x\text{FeMoO}_6$ series, although La^{3+} radius ($r_{\text{La}^{3+}} = 1.36 \text{ \AA}$) is smaller than that of Sr^{2+} ($r_{\text{Sr}^{2+}} = 1.44 \text{ \AA}$) an increase in lattice parameters with increasing La content is observed [4]. This can be explained due to lowering of valence state of cations ($r_{\text{Fe}^{2+}} = 0.78 \text{ \AA}$ compared to $r_{\text{Fe}^{3+}} = 0.785 \text{ \AA}$ or $r_{\text{Mo}^{4+}} = 0.65 \text{ \AA}$ compared to $r_{\text{Mo}^{5+}} = 0.61 \text{ \AA}$) to satisfy the charge neutrality condition when Sr^{2+} is replaced by La^{3+} . Similar trend is found for the $\text{Sr}_2\text{Fe}_{1-x}\text{Zn}_x\text{MoO}_6$ series which is attributed to the large radius of Zn^{2+} ion, $r_{\text{Zn}^{2+}} = 0.88 \text{ \AA}$ compared to $r_{\text{Fe}^{3+}} = 0.785 \text{ \AA}$ and $r_{\text{Mo}^{5+}} = 0.75 \text{ \AA}$ [8]. The average crystallite size D was obtained by analysis of the peak broadening. The crystallite size is distributed in nanoscale from 31-38 nm and 31-54 nm for the $\text{Sr}_{2-x}\text{La}_x\text{FeMoO}_6$ and $\text{Sr}_2\text{Fe}_{1-x}\text{Zn}_x\text{MoO}_6$ series, respectively.

The grain size and morphology of the samples were characterized by FESEM. The results show that the samples are in form of clusters which compose of many tiny grains in range 20-60 nm. This observation is in agreement with the broadening of the diffraction peaks in XRD patterns. It can be concluded that under the preparation conditions, the growth of small grains to bigger ones is hindered and nanocrystalline structures are retained in the samples.

Table 1. Antisite disorder p , magnetic moment in the ground state m_0 and Curie temperature T_C of the $\text{Sr}_{2-x}\text{La}_x\text{FeMoO}_6$ and $\text{Sr}_2\text{Fe}_{1-x}\text{Zn}_x\text{MoO}_6$ series.

| $\text{Sr}_{2-x}\text{La}_x\text{FeMoO}_6$ | | | |
|---|---------|-------------------------------|-----------|
| x | p (%) | m_0 ($\mu_B/\text{f.u.}$) | T_C (K) |
| 0 | 20 | 2.34 | 420 |
| 0.1 | 19 | 2.36 | 416 |
| 0.2 | 22 | 2.08 | 410 |
| 0.3 | 32 | 1.32 | 426 |
| 0.4 | 35 | 1.09 | 428 |
| $\text{Sr}_2\text{Fe}_{1-x}\text{Zn}_x\text{MoO}_6$ | | | |
| x | p (%) | m_0 ($\mu_B/\text{f.u.}$) | T_C (K) |
| 0.05 | 19 | 2.25 | 409 |
| 0.1 | 17 | 2.18 | 404 |
| 0.15 | 15 | 2.17 | 398 |

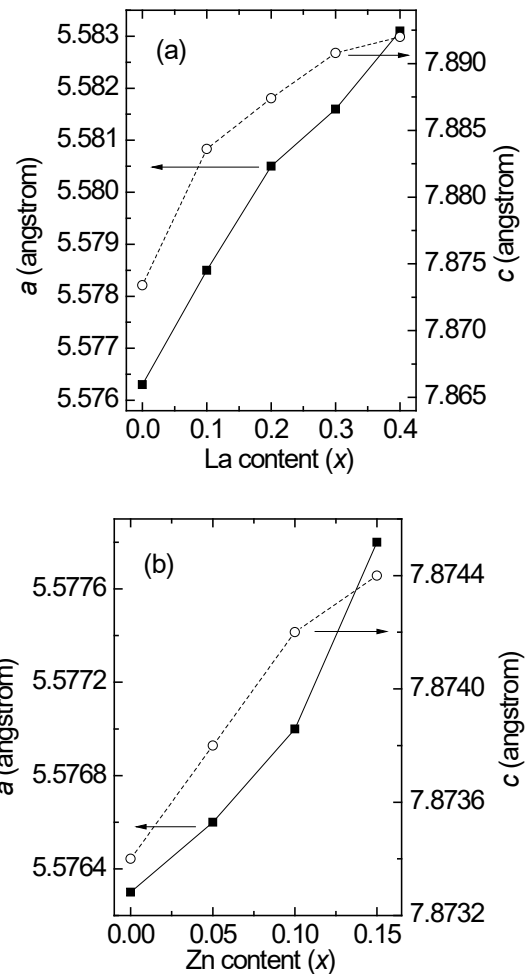


Fig. 1. Evolution of lattice parameters a and c of the $\text{Sr}_{2-x}\text{La}_x\text{FeMoO}_6$ (a) and $\text{Sr}_2\text{Fe}_{1-x}\text{Zn}_x\text{MoO}_6$ (b) series.

The magnetization curves of the samples were measured in the temperature range between 88 and 430 K. The magnetization curves measured at 88 K of the two series are shown in Fig. 2. For all cases, the magnetization increases steeply in the low-field part

of the curve and then increases linearly with further increasing field. The linear part of the $M-H$ curves starts in applied fields of ~ 4 kOe. The high-field susceptibility χ_{HF} is closely related to the occupancy of Fe ions in the B' sites. When Fe ions occupy the B' site, antiferromagnetic coupling $Fe^{B-O}-Fe^{B'}$ is created, leading to a reduction of the total magnetization compared to highly order structure. By applying a magnetic field, antiparallel Fe moments are forced to align to the field direction and hence a high-field susceptibility appears. Another source for χ_{HF} and a reduction of spontaneous magnetization can also be found in disordered spins at the surface region of the nanoparticles.

The χ_{HF} values of the magnetization curves were determined as the slope of the linear part in high field. All the magnetization curves can be reconstructed using the following equation:

$$M(H) = M_s(1 - \exp(-H/a)) + \chi_{HF}H \quad (1)$$

where the saturation magnetization, M_s , and a are fitting parameters. The first term describes the magnetization originated from the ferrimagnetic order of the core spin and itinerant moments which saturates in high field and the second term is the susceptibility contribution. The fitting curves are also plotted together with the experimental data (Fig. 2). The saturation magnetization values of the samples determined in the investigated temperature range are shown in Fig. 3. It is seen that in the temperature region up to about half of the Curie temperature, M_s decreases linearly as temperature increases and then drop more drastically as temperature approaches T_C . This behavior is consistent with the results derived from band structure calculations for the SFMO material by Erten *et al.* [9]. The M_s values at 0 K, $M_s(0)^{ext}$, for the samples were determined by extrapolating the linear part of the M_s vs. T curves down to zero Kelvin. From these values, the net magnetic moment at 0 K, m_0 , was calculated as $M_s(0)^{ext} \times W / 5585 (\mu_B/f.u.)$ for the samples, where W is molar mass. As seen in Table 1, the m_0 values derived for these samples are far below the value for the perfectly ordered structure ($4 \mu_B/f.u.$). For pure SFMO ($x = 0$), the dependence of m_0 on antisite fraction, p , is described as follows:

$$m_0 = 4 - 8p. \quad (2)$$

This formula was justified by the experimental data [10] and the Monte Carlo computation [11] based on the assumption of the antiferromagnetic coupling of $Fe^{B-O}-Fe^{B'}$ and no magnetic coupling in $Mo^{B-O}-Mo^{B'}$.

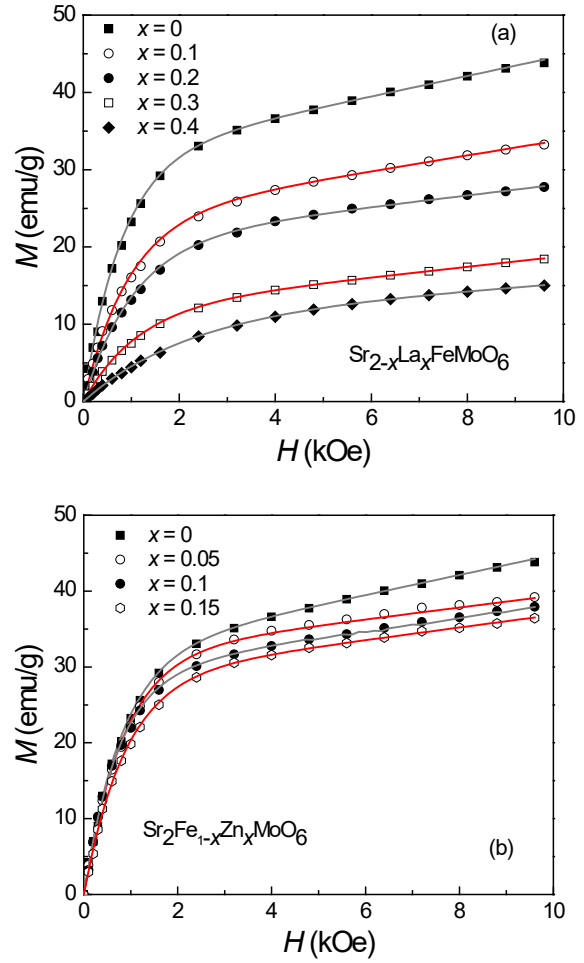


Fig. 2. The magnetization curves measured at 88 K for the $Sr_{2-x}La_xFeMoO_6$ (a) and $Sr_2Fe_{1-x}Zn_xMoO_6$ (b) series. Lines are fitting curves according to eq. (1) (see text).

In the case of $Sr_{2-x}La_xFeMoO_6$, as La^{3+} replaces Sr^{2+} , a net electron doping at the Fermi level takes place. Consequently, the higher band filling increases the density of states at the Fermi level, which would strengthen the Fe/Mo double exchange mechanism [55DP]. As observed in Table 1, the saturation magnetization strongly decreases with $x \geq 0.2$. This decrease is attributed to two different effects. First, due to the antiparallel coupling of the added electron with the local magnetic moment, m_0 , will diminish according to the dependence $[5 - (1 + x)] \mu_B/f.u.$ Second, the presence of AS reduces the magnetization as given by Eq. 2. As long as the gap at the Fermi level in the spin down conduction band is preserved, every added electron will contribute with $-1 \mu_B/f.u.$, even in presence of AS. Hence, Eq. (2) transforms to:

$$m_0 = 4 - 8p - x. \quad (3)$$

However, it has been shown that AS disorder gradually destroys the half-metallic character of the electronic structure [13,14]. For instance, ab initio calculations show that for a crystal structure with AS = 25%, the DOS retains a negative spin polarization of only ~33% [13]. In the limit of AS = 50%, the spin polarization should vanish. An alternative way to Eq. (3) to allow for this effect is to assume that every antisite promotes an available spin up state at the conduction band. Then, as done in the case of $\text{Sr}_{2-x}\text{La}_x\text{FeMoO}_6$ [15], Eq. (2) transforms to:

$$m_0 = (4 - x)(1 - 2p). \quad (4)$$

The antisite disorder parameter, p , was calculated for the La substituted series according to Eq. (4) and is shown in Table 1. It is seen that the antisite level of the sample $x = 0.1$ is a bit less than that of the pure SFMO sample but it increases drastically from 22% to 35% as x increases from 0.2 to 0.4.

The Curie temperature of the samples was determined as temperature at which M_s vanishes (Table 1). The results show that for the pure SFMO, although the AS level is as high as 20%, the Curie temperature is still comparable to that of the ordered structure ($T_C = 420$ K). For the $\text{Sr}_{2-x}\text{La}_x\text{FeMoO}_6$ series, in principle, the injection of carriers into the system would promote an enhancement of the ferromagnetic correlations. However for $x = 0.1$ and 0.2, a decrease of T_C is found because the steric effect [3] also play a role. This effect comes from the substitution of Sr^{2+} by La^{3+} , which is accompanied by an expansion of the cell volume and a distortion of the oxygen octahedra. This, in turn, traduces in larger bond distances and smaller bond angles which are known to diminish the ferromagnetic interaction strengths when these are mediated by itinerant carriers. Furthermore, it has been pointed out [16] that doping electrons tend to localize in Mo orbitals for $x < 0.3$. For $x = 0.3$ and 0.4, the Curie temperature substantially increases indicating the dominance of band filling effect.

In the case of $\text{Sr}_2\text{Fe}_{1-x}\text{Zn}_x\text{MoO}_6$, according to the equation of $\text{Fe}^{3+} + \text{Mo}^{5+} \rightarrow \text{M}^{2+} + \text{Mo}^{6+}$, the doped Zn^{2+} ions can induce the formation of Mo^{6+} . So the nonmagnetic $\text{Zn}^{2+}\text{-O-Mo}^{6+}$ pairs may exist in $\text{Sr}_2\text{Fe}_{1-x}\text{Zn}_x\text{MoO}_6$. Assuming the case that all Zn ions located at the normal Fe site (B site), and thus the value of m_0 of the $\text{Sr}_2\text{Fe}_{1-x}\text{Zn}_x\text{MoO}_6$ series can be given as:

$$m_0 = 4 - 8p - 4x, \quad (5)$$

where the second term corresponds to the reduction of magnetization due to the formation of nonmagnetic $\text{Zn}^{2+}\text{-O-Mo}^{6+}$ pairs.

The antisite disorder parameter, p , determined from Eq. (5), decreases monotonically with increasing Zn content (Table 1). This result can be attributed to the increase of the order of the B/B' sublattice as the charge difference between B and B' sites increases [17,18]. Also, due to the Zn substitution which results in the removal of itinerant carriers from the conduction band and the degradation of ferromagnetism in the series, the Curie temperature is found to decrease with increasing Zn content.

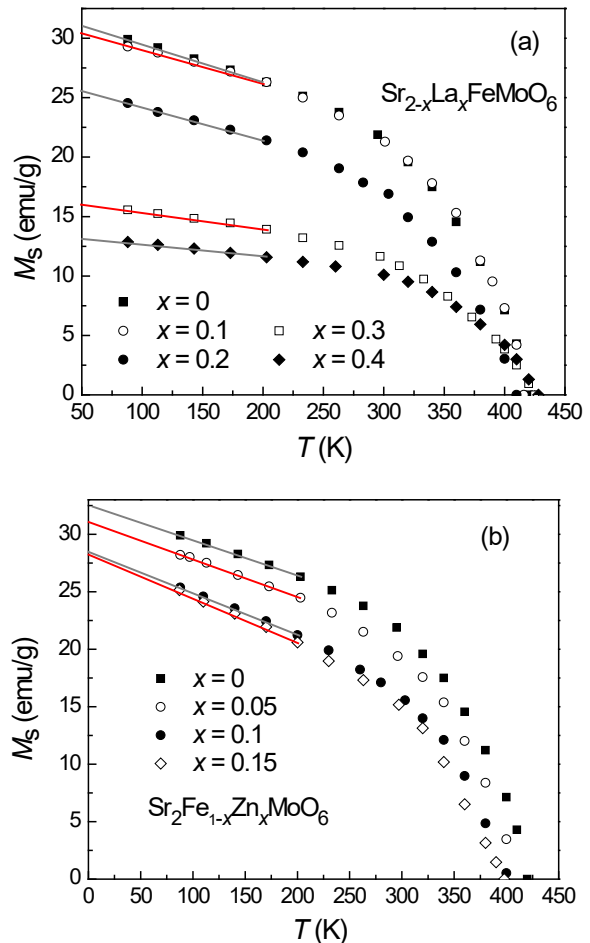


Fig. 3. Spontaneous magnetization M_s as a function of temperatures for the $\text{Sr}_{2-x}\text{La}_x\text{FeMoO}_6$ (a) and $\text{Sr}_2\text{Fe}_{1-x}\text{Zn}_x\text{MoO}_6$ (b) series. Solid lines are extrapolation to zero Kelvin.

4. Conclusion

The La and Zn substituted SFMO double perovskites were fabricated using a sol-gel technique in combination with heat treatment at 1100°C. For both substituted series, the magnetic moment at 0 K decreases with increasing the substitution levels. For the La substituted samples with low substitution levels, $x = 0.1$ and 0.2, the Curie temperature

decreases compared to the pure SFMO which is attributed to the dominance of the steric effect while it increases for $x = 0.3$ and 0.4 in which the band filling takes the prevailing role. For the Zn substituted samples, T_C decreases monotonically with increasing the Zn content which is attributed to the lowering of electron density in the conduction band upon Zn substitution. Based on the magnetic moment m_0 , the antisite disorder was estimated for the samples. High AS level of 20% was introduced in the pure sample due to low annealing temperature. The degree of AS increases with increasing La substitution level whilst it decreases with increasing the Zn content. The experimental data also shows that the magnetic ordering temperature is not sensitive to AS.

Acknowledgments

This research is funded by the Hanoi University of Science and Technology (HUST) under project number T2017-PC-175.

References

- [1] K. I. Kobayashi, T. Kimura, H. Sawada, K. Terakura; Room-temperature magnetoresistance in an oxide material with an ordered double-perovskite structure; *Nature (London)* 395 (1998) 677.
- [2] J. Navarro, C. Frontera, Ll. Balcells, B. Martínez, and J. Fontcuberta; Raising the Curie temperature in $\text{Sr}_2\text{FeMoO}_6$ double perovskites by electron doping; *Phys. Rev. B* 64 (2001) 092411.
- [3] D. Sánchez, J.A. Alonso, M. García-Hernández, M.J. Martínez-Lope, M.T. Casais, J.L. Martínez, M.T. Fernández-Díaz; Electron and hole doping effects in $\text{Sr}_2\text{FeMoO}_6$ double perovskites; *J. Magn. Magn. Mater.* 272–276 (2004) 1732–1733.
- [4] G. Narsinga Rao, Saibal Roy, Chung-Yuan Mou, J.W. Chen; Effect of La doping on magnetotransport and magnetic properties of double perovskite $\text{Sr}_2\text{FeMoO}_6$ system; *J. Magn. Magn. Mater.* 299 (2006) 348–355.
- [5] E.K. Hemery, G.V.M. Williams, H.J. Trodahl; Isoelectronic and electronic doping in $\text{Sr}_2\text{FeMoO}_6$; *J. Magn. Magn. Mater.* 310 (2007) 1958–1960.
- [6] Min Feng Lü, Jing Ping Wang, Jian Fen Liu, Wei Song, Xian Feng Hao, De Feng Zhou, Xiao Juan Liu, Zhi Jian Wu and Jian Meng; An investigation of low-field magnetoresistance in the double perovskites $\text{Sr}_2\text{Fe}_{1-x}\text{Zn}_x\text{MoO}_6$, $x = 0, 0.05, 0.15$ and 0.25 ; *J. Phys.: Condens. Matter* 18 (2006) 1601–1612.
- [7] Xianjie Wang, Yu Sui, Qiuli Yang, Jinguang Cheng, Zhengnan Qian, Zhiguo Liu, Wenhui Su; Effect of doping Zn on the magnetoresistance of polycrystalline $\text{Sr}_2\text{FeMoO}_6$; *J. Alloys Compd.* 431 (2007) 6–9.
- [8] R.D. Shannon; Revised effective ionic radii and systematic studies of interatomic distances in halides and chalcogenides; *Acta Crystallogr. A* 32 (1976) 751.
- [9] O.N. Meetei, O. Erten, A. Mukherjee, M. Randeria, N. Trivedi, P. Woodward; Theory of half-metallic double perovskites. I. Double exchange mechanism; *Phys. Rev. B* 87 (2013) 1–7.
- [10] Ll. Balcells, J. Navarro, M. Bibes, A. Roig, B. Martínez, J. Fontcuberta; Cationic ordering control of magnetization in $\text{Sr}_2\text{FeMoO}_6$ double perovskite; *Appl. Phys. Lett.* 78 (2001) 781.
- [11] A.S. Ogale, S.B. Ogale, R. Ramesh, T. Venkatesan; Octahedral cation site disorder effects on magnetization in double-perovskite $\text{Sr}_2\text{FeMoO}_6$; Monte Carlo simulation study; *Appl. Phys. Lett.* 75 (1999) 537.
- [12] P. Schiffer, A.P. Ramirez, W. Bao, S.W. Cheong; Low Temperature Magnetoresistance and the Magnetic Phase Diagram of $\text{La}_{1-x}\text{Ca}_x\text{MnO}_3$; *Phys. Rev. Lett.* 75 (1995) 3336–9.
- [13] T. Saha-Dasgupta, D.D. Sarma; Ab initio study of disorder effects on the electronic and magnetic structure of $\text{Sr}_2\text{FeMoO}_6$; *Phys. Rev. B* 64 (2001) 064408.
- [14] D. Stoeffler, S. Colis; Oxygen vacancies or/and antisite imperfections in $\text{Sr}_2\text{FeMoO}_6$ double perovskites: an ab initio investigation; *J. Phys.: Condens. Matter* 17 (2005) 6415–24.
- [15] J. Navarro, J. Fontcuberta, M. Izquierdo, J. Avila, M.C. Asension; Curie-temperature enhancement of electron-doped $\text{Sr}_2\text{FeMoO}_6$ perovskites studied by photoemission spectroscopy; *Phys. Rev. B* 69 (2004) 115101.
- [16] Y. Moritomo, Sh. Xu, T. Akimoto, A. Machida, N. Hamada, K. Ohoyama, E. Nishibori, M. Takata, M. Sakata; Electron doping effects in conducting $\text{Sr}_2\text{FeMoO}_6$; *Phys. Rev. B* 62 (2000) 14224.
- [17] D. Rubi, C. Frontera, J. Nogués, J. Fontcuberta; Enhanced ferromagnetic interactions in electron doped $\text{Nd}_x\text{Sr}_{2-x}\text{FeMoO}_6$ double perovskites; *J. Phys. Condens. Mater.* 16 (2004) 3173.
- [18] C.L. Yuan, Y. Zhu, P.P. Ong; Enhancement of room-temperature magnetoresistance in $\text{Sr}_2\text{FeMoO}_6$ by reducing its grain size and adjusting its tunnel-barrier thickness; *J. Appl. Phys.* 91 (2002) 4421.